

# Evaluation of Prestressed Concrete Bridges under Light Rail Loading

by Yail J. Kim and Yongcheng Ji

*This paper presents the evaluation of prestressed concrete bridges carrying light rail loading, which is significantly unexplored relative to bridges subjected to conventional heavy-haul and high-speed trains. Four bridges in Denver, CO, are selected to investigate static and dynamic responses, including flexural behavior, passenger occupancy, statistical properties, live load distributions, natural frequencies, and user comfort. Three-dimensional finite element models are developed to complement in-place findings. The measured train loadings are statistically stable along with Gaussian distributions and increase by 10.8% when their average operating speed rises from 32.9 to 49.0 mph (53 to 78 kmh). Passenger loading that is stochastic in nature also increases the train loading by 23.3%, on average. Existing design approaches for live load distributions deviate from those attained from the field, which is particularly noticeable for interior girders. Deflection control criteria used in practice are not applicable either. In accordance with the deflection and frequency of the bridges, the user comfort of light rail systems (pedestrians and passengers) is assessed. Statistical properties are acquired and characterized, which are valuable when developing design guidelines.*

**Keywords:** bridge; evaluation; light rail transit; live load; modeling.

## INTRODUCTION

Light rail systems are a salient transportation component in urban communities. According to the American Public Transportation Association,<sup>1</sup> light rail transit is defined as “An electric railway system characterized by its ability to operate single or multiple cars along exclusive rights-of-way at ground level, on aerial structures, in subways or on streets, able to board and discharge passengers at station platforms or at street, track, or car-floor level and normally powered by overhead electrical wires.” Owing to the convenient operation and environmental friendliness (electrically propelled without emission), light rail transit has been adopted by most major cities in the United States. The transit system in Washington, for instance, carries over 600,000 passengers daily.<sup>2</sup> Despite light rail trains’ prevalence, their loading characteristics and corresponding effects were not sufficiently reported. The majority of literature on rail bridges is concerned with conventional heavy-haul trains and high-speed trains,<sup>3–5</sup> while a few conference papers have been published on the in-place monitoring of light rail bridges. Yuan et al.<sup>6</sup> examined the behavior of prestressed concrete bridges (I-shape and box girders) subjected to light rail trains; however, the focus was on substructural responses. Khan et al.<sup>7</sup> reported a preliminary field monitoring project with a bridge carrying light rail trains. The bridge consisted of four simply supported prestressed concrete girders at an average span of 95 ft (29 m). Strain transducers and acceler-

ometers were installed beneath the upper and lower flanges of the girders. The measured dynamic load allowance was lower than the design values of the American Association of State Highway Transportation Officials (AASHTO) Load and Resistance Factor Design (LRFD) Bridge Design Specifications (BDS)<sup>8</sup> and the American Railway Engineering and Maintenance-of-Way Association (AREMA) manual.<sup>9</sup> The field-monitored live load distributions deviated from those calculated by the Lever Rule method, which is frequently used in practice, although detailed discussions were missing. According to these limited investigations, current design approaches may not reflect the actual behavior of light rail bridges and thus may need comprehensive assessment and improvement. As a first step to propose design recommendations or revise specifications, the implications of light rail trains on the behavior of bridges should be monitored, evaluated, and elucidated.

This paper discusses the in-place evaluation of light rail bridges, followed by three-dimensional finite element modeling. The objectives of the study are 1) to understand the loading and influence of light rail transit on the static and dynamic responses of prestressed concrete bridges; and 2) to assess the applicability of existing design approaches. In addition to response monitoring with strain gauges, a state-of-the-art technique (interferometric radar) is employed to measure the dynamic deflection of the bridges (displacement measurement requires more effort than strain recording in rail bridges; hence, the former is rarely exploited on site<sup>10</sup>). Specific interests involve flexural responses, passenger occupancy, statistical properties, live load distributions, natural frequencies, and user comfort.

## RESEARCH SIGNIFICANCE

The behavior of light rail bridges is limitedly known; consequently, practice is based on AASHTO LRFD BDS, the AREMA manual, and agency-specific design guidelines. The articles of AASHTO LRFD BDS and AREMA, however, do not represent responses resulting from light rail transit, and most agency-specific guidelines have been empirically developed without experimental/field validation. It is, therefore, unclear how light rail trains generate structural loadings to bridges and how much discrepancy is associated with the existing specifications. The present

*ACI Structural Journal*, V. 116, No. 1, January 2019.

MS No. S-2017-458, doi: 10.14359/51706921, was received November 28, 2017, and reviewed under Institute publication policies. Copyright © 2019, American Concrete Institute. All rights reserved, including the making of copies unless permission is obtained from the copyright proprietors. Pertinent discussion including author’s closure, if any, will be published ten months from this journal’s date if the discussion is received within four months of the paper’s print publication.

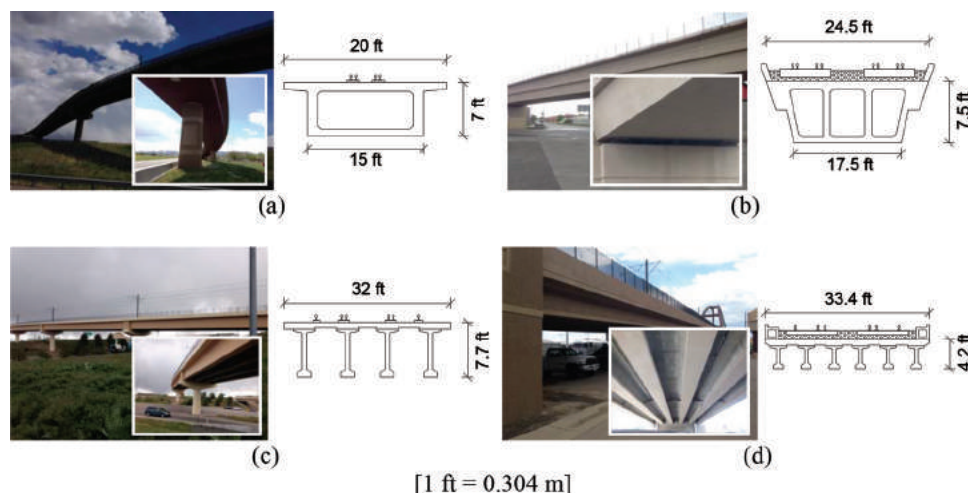


Fig. 1—Prestressed concrete bridges carrying light rail transit: (a) Indiana Bridge; (b) Santa Fe Bridge; (c) County Line Bridge; and (d) 6th Avenue Bridge.

research deals with the evaluation of prestressed concrete bridges loaded by light rail trains in Denver, CO, as well as data interpretation for the appraisal of design approaches, including the characterization of statistical properties.

## BACKGROUND OF PRESTRESSED CONCRETE BRIDGES

A total of four constructed bridges in Denver, CO, are monitored. These bridges have been in service for 7 to 13 years. The monitored span of the individual bridges is determined by the following criteria as recommended by the Regional Transportation District (RTD) that controls all light rail transit systems in Denver: 1) lowest superstructure elevation for safety; and 2) accessibility to tracks with minimal disruption to train operation. Prior to conducting response monitoring, the site condition of these bridges has been evaluated (Fig. 1). The purposes of the site visit are to identify potential problems that might influence technical work, and to confirm engineering drawings obtained from RTD. A plan for instrumentation is established (Appendix A\*). Typical field monitoring time is 12 hours from 8:00 am to 8:00 pm per bridge; however, 2 days are spent for one bridge owing to a strong wind issue. The behavior of the bridges is converged from a statistics perspective, which means there is no practical need to extend the monitoring time (that is, sufficient data have been obtained). Train speed was measured with a digital speed gun confirmed by a portable global positioning system (GPS) inside trains passing the bridges.

### Bridge details

**Indiana Bridge**—The Indiana Bridge has no skew and is composed of a hollow prestressed concrete box girder with a direct fixation track (Fig. 1(a)). The depth and width of the box girder are 7 and 20 ft (2.1 and 6.1 m), respectively, and the 28-day compressive strength of the girder concrete was 5800 psi (40 MPa). Post-tensioning was conducted with

low-relaxation steel strands ( $A_{ps} = 28.64 \text{ in.}^2 [18,480 \text{ mm}^2]$  and  $f_{pu} = 270 \text{ ksi [1860 MPa]}$ , where  $A_{ps}$  and  $f_{pu}$  are the cross-sectional area and ultimate strength of the steel, respectively) at a jacking stress level of  $75\%f_{pu}$ . The monitored span is 95 ft (29 m) long and has expansion and fixed bearings at both ends (Fig. 2(a)). Instrumentation included 1) eight strain gauges bonded to the rail-side to measure in-place train wheel load (Fig. 2(b)); 2) one strain gauge bonded in between the strain gauge clusters for temperature monitoring; and 3) nine strain gauges (three 4.7 in. [120 mm] gauge-length and six 0.2 in. [5 mm] gauge-length gauges) bonded to the bottom of the girder (Fig. 2(c)) to monitor the flexural response of the bridge at midspan (bending and live load distribution). Unlike other bridges monitored in this research program, one-way travel is allowed along the single track and light rail trains are alternatively operated from Denver to Golden, CO (east to west) and vice versa, as shown in Fig. 2(d).

**Santa Fe Bridge**—The Santa Fe Bridge is a two-span multi-cell prestressed concrete box girder bridge (Fig. 1(b)). The bridge is approximately 28 ft wide (8.5 m) and 10 ft deep (3 m), and has a total length of 328 ft (100 m) (172 ft [52 m] + 156 ft [48 m] spans). Two train tracks are located on a ballast layer of 1.7 ft (0.52 m). The 28-day compressive strength of the box concrete was 6000 psi (41 MPa), and low-relaxation strands ( $A_{ps} = 76 \text{ in.}^2 [49,030 \text{ mm}^2]$  and  $f_{pu} = 270 \text{ ksi [1860 MPa]}$ ) were used for post-tensioning at a jacking stress level of  $75\%f_{pu}$ . Strain gauges were bonded to the rail side to measure train load and temperature and were bonded underneath each web member of the multi-cell girder, as in the case of the Indiana Bridge.

**County Line Bridge**—The County Line Bridge ( $L = 990 \text{ ft [300 m]}$ ) comprises four prestressed concrete bulb-tee girders (Colorado BT84) for seven spans varying from 114 to 160 ft (35 to 49 m), as shown in Fig. 1(c). Each girder has a depth of 7 ft (2.1 m) with a girder spacing of 8.3 ft (2.5 m), and supports a deck slab ( $t = 8 \text{ in. [200 mm]}$ ) with two direct-fixation tracks. All girders were connected by diaphragms cast on site (a continuous system), except the fourth span, where expansion joints were placed. Two harping points were used for prestressing strands per girder ( $A_p = 5.2 \text{ to } 12.6 \text{ in.}^2 [3360 \text{ to } 8130 \text{ mm}^2]$ ),

\*The Appendix is available at [www.concrete.org/publications](http://www.concrete.org/publications) in PDF format, appended to the online version of the published paper. It is also available in hard copy from ACI headquarters for a fee equal to the cost of reproduction plus handling at the time of the request.

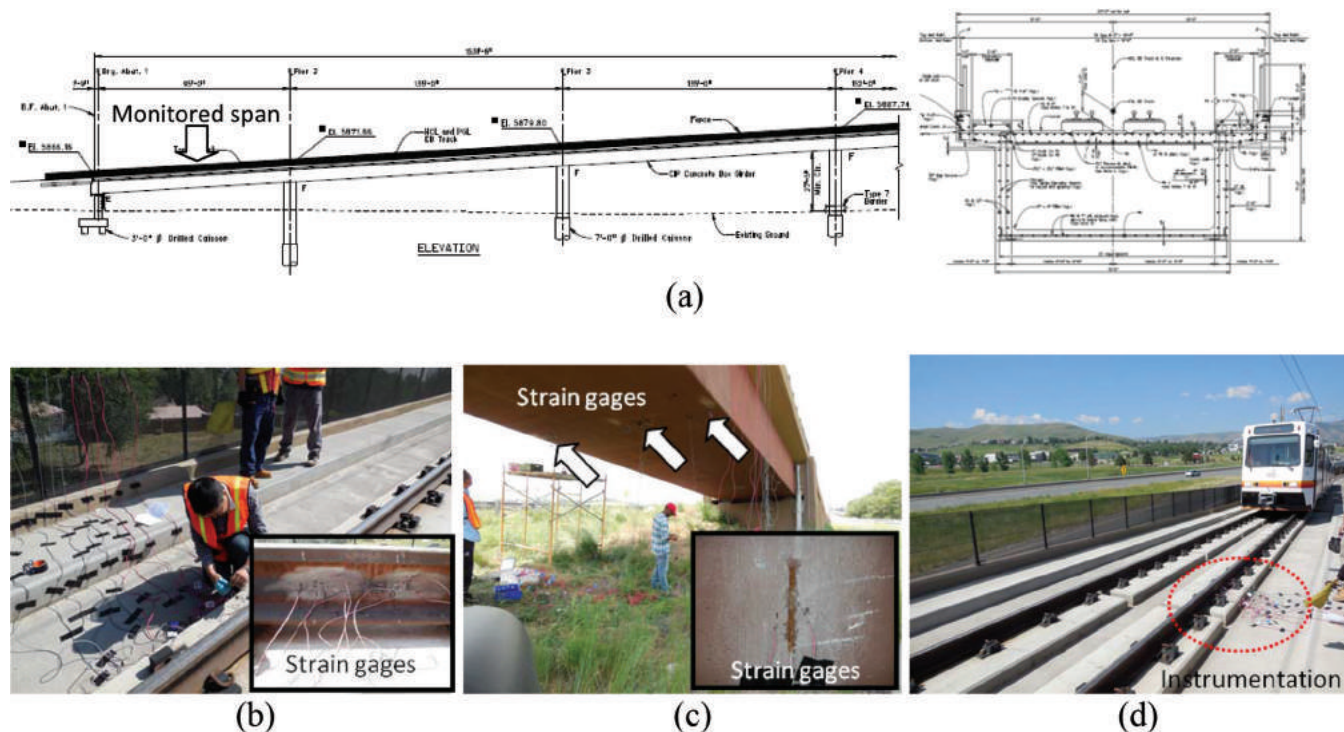


Fig. 2—Instrumentation for rail and superstructure responses (Indiana Bridge): (a) elevation view and typical cross section of girder; (b) rail gauge bonding; (c) girder gauges; and (d) one-way train track.

low-relaxation 270 ksi [1860 MPa] steel). A 28-day concrete strength of 8500 psi (60 MPa) was used for the girders. Strain gauges were bonded to the rail to measure light rail train load. Additional gauges were bonded to the bottom of each girder at midspan to monitor the flexural behavior when loaded.

**6th Avenue Bridge**—The 6th Avenue Bridge has 4 + 2 span prestressed concrete bulb-tee girders (BT42) connected by an arch bridge (Fig. 1(d)). The non-skew bridge encompasses two ballasted train tracks. A waterproofing membrane layer was placed in between the deck concrete ( $t = 8$  in. [200 mm]) and the ballast layer. Similar to the County Line Bridge, all girders were connected on site to make a continuous system, and each girder had two harping points ( $A_p = 5.2$  in.<sup>2</sup> [3350 mm<sup>2</sup>] with an effective steel stress of  $56\%f_{pu}$ ). The compressive strength of the girder concrete was 9000 psi (62 MPa). Strain gauges were bonded like other bridges to measure the in-place wheel load of light rail trains and the flexural response of the girders at midspan.

### Calibration of rail response

A laboratory experiment was conducted to calibrate the response of a 115RE rail under mechanical loading. A 128-in. (3.3-m) long rail was tested with strain gauges, as shown in Fig. 3(a) to (c). The strain gauge configuration used is similar to the method recommended by the Association of American Railroads (AAR) for wheel load calibration, which is frequently implemented in practice.<sup>11</sup> Figures 3(d) and (e) exhibit the load-strain behavior of the 115RE rail. Two loading conditions were employed: simply supported and continuous. According to the RTD design manual,<sup>12</sup> the front wheel of a fully loaded train weighs 12.2 kip (54 kN) ('Full train' in Fig. 3), whereas that of an empty train is 7.5 kip (33 kN) ('Empty train' in Fig. 3). The

strains measured at the bottom of the rail where a maximum flexural effect takes place were compared with those calculated by structural analysis formulas. The strain values of the continuous rail were less than those of the simply supported case (for example, the measured strain of the continuous rail was 39% less than that of its simply supported counterpart at a load of 7.5 kip [33 kN]). This observation indicates that the proposed test setup can properly represent the response of continuous rails supported by multiple sleepers on site. The response of the strain gauges bonded to the rail side is given in Fig. 4(a). The gauges facing each other in the diagonal direction showed similar behavior. Test data revealed slight discrepancy between the G1/G3 and G2/G4 groups, which illustrates that the applied principle stresses in these two diagonal directions (that is,  $\sigma_1$  and  $\sigma_2$ ) were not the same. Linear curve-fitting equations were developed to establish the relationship between the strain and the applied load, so that in-place train load would be measured based on strain reading. Figure 4(b) shows the calibration of a portable data acquisition system using a conventional laboratory data acquisition system. At typical loads of 12 and 14 kip (53 and 62 kN) in the continuous rail test, the strain reading of these two systems was almost identical. These calibration results corroborate that the use of the portable data acquisition system is adequate to measure the in-place behavior of the four bridges discussed earlier. The established load-strain relationships were further validated with actual train load on site (Fig. 4(c)). The front wheel of an empty stationary train (7.5 kip [33 kN]) generated a maximum strain of 64.5 microstrains, as shown in Fig. 4(d), which agreed with the laboratory strain of 63.8 microstrains subjected to the same load magnitude (only one gauge reading is provided for clarity).



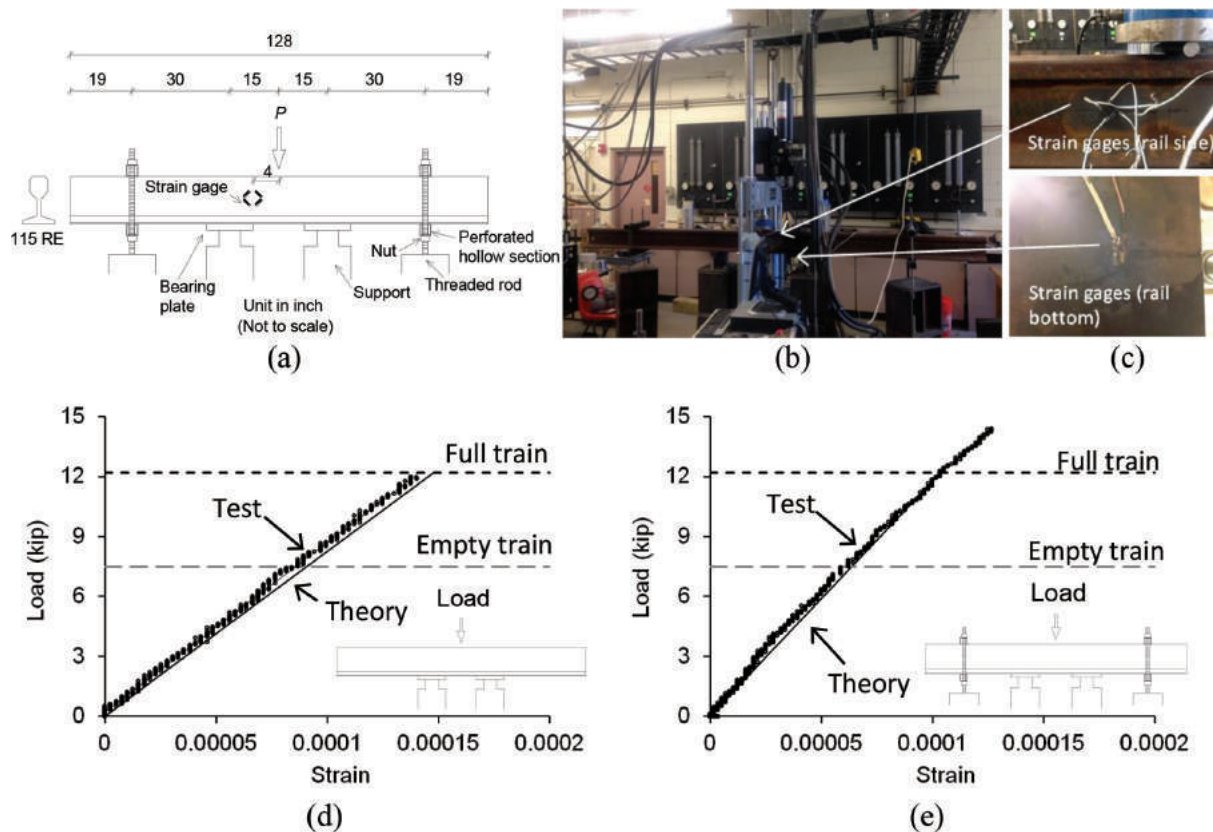


Fig. 3—Test details for response calibration: (a) schematic (unit in inch); (b) experimental setup; (c) strain gauge configurations for the side and bottom of rail; (d) behavior at bottom of rail in simply supported case; and (e) behavior at bottom of rail in continuous case. (Note: 1 kip = 4.448 kN; 1 in. = 25.4 mm.)

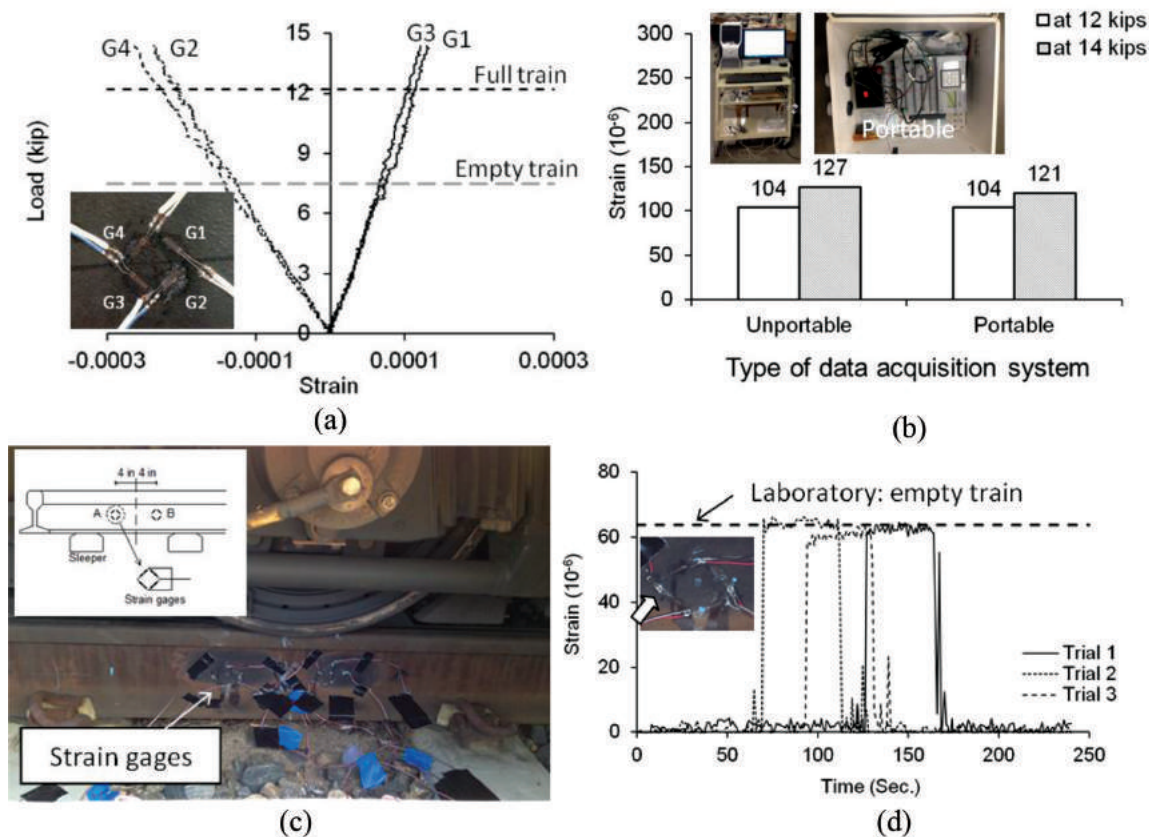


Fig. 4—Load-strain behavior on side of continuous rail: (a) strain response; (b) comparison of data acquisition systems; (c) wheel positioning; and (d) comparison between in-place test and laboratory test (front wheel load). (Note: 1 kip = 4.448 kN; 1 in. = 25.4 mm.)

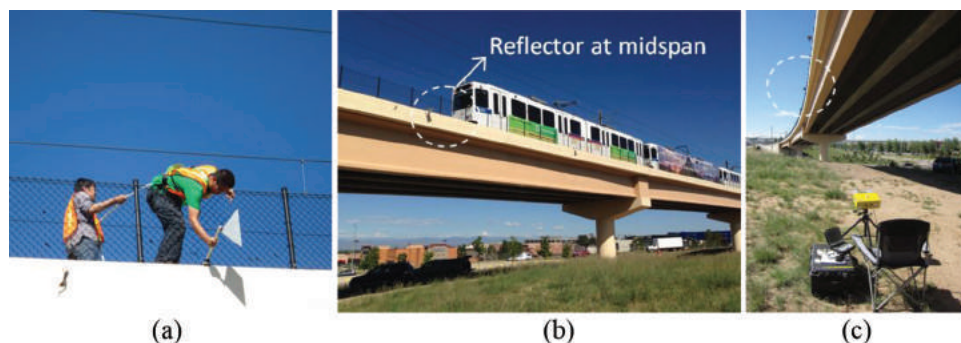


Fig. 5—Non-contact interferometric radar technique for measuring dynamic behavior of County Line Bridge: (a) installation of reflector; (b) trains passing; and (c) IBIS setup for monitoring.

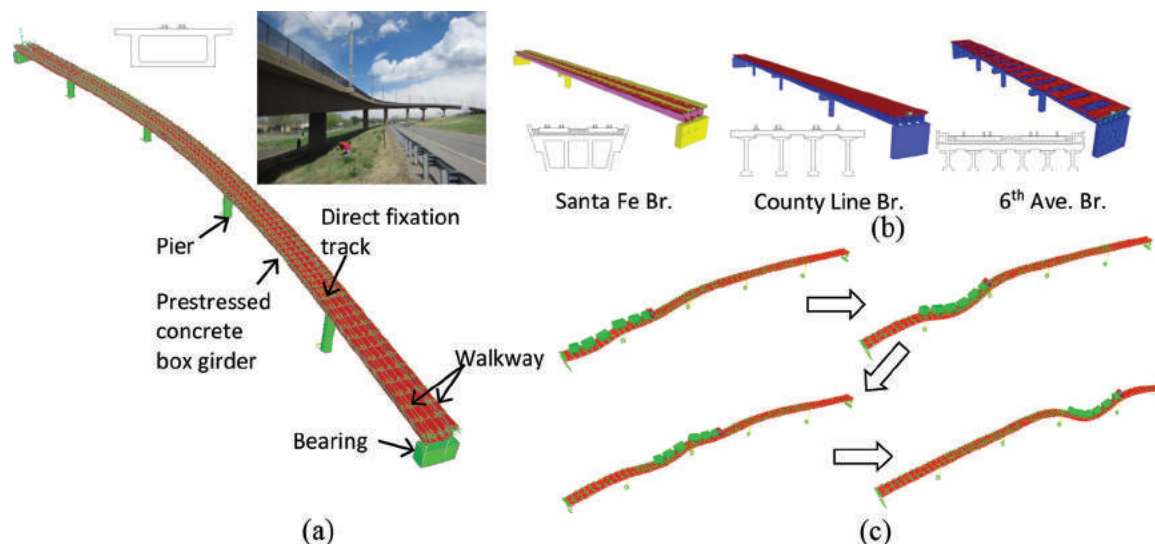


Fig. 6—Developed bridge models: (a) Indiana Bridge (five spans: 628 ft [191 m]); (b) other bridges; and (c) behavior of Indiana Bridge subjected to two articulated light rail trains at speed of 40.4 mph (65 kmh).

### Monitoring of dynamic response

A non-contact interferometric radar technique called Image By Interferometric Survey (IBIS hereafter) was employed to monitor the dynamic behavior of the bridges. The IBIS system detects a phase-change in reflected radar waves to identify the position of an object at an accuracy of 0.0002 to 0.004 in. (0.005 to 0.1 mm). Reflectors were installed along the edge of the bridge deck at mid- and quarterspans (Fig. 5(a) and (b)) to measure the displacement and frequency of the bridge. The monitored spans were identical to those of the previously mentioned field test. The IBIS equipment was set up using a tripod, as shown in Fig. 5(c), and the radar head was connected to a laptop computer. A laser distance meter mounted to the radar head was used to uniquely link the position of specific bridge members with a peak radar display. This process enabled reviewing in-place technical data at a later time for further data processing such as Fast Fourier Transform (FFT) analysis. A sampling rate of 200 Hz was exploited. Using the IBIS system, the vibration and displacement data of all four bridges were collected and analyzed.

### FINITE ELEMENT MODELING

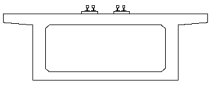
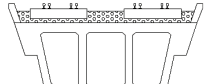
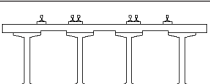
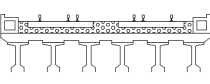
After careful examination and trial modeling, CSI Bridge and SAP2000 finite element programs were selected, in

addition to their familiarity, convenience, popularity, and accuracy in bridge modeling. Figure 6 illustrates bridge models to predict field test data. The following properties were considered per the engineering drawings and documents obtained from RTD, as summarized in Table 1:

- Superstructure types: prestressed concrete girders and prestressed concrete box girders
- Geometric details: depth, width, and length of the girders, rail-supporting plinths, sidewalks, and diaphragms
- Material properties: concrete, steel strands, and ballast
- Live load: empty and fully-loaded light rail trains (total load = 79 and 130 kip [351 and 578 kN], respectively, per one articulated train [to be detailed])
- Number of articulated light rail trains: two to three articulated light rail trains, as observed on site
- Operating speed of light rail trains: average speeds measured on site
- Boundary conditions: hinges and rollers

The average operating speeds of the light rail trains for the 6th Avenue Bridge (32.9 mph [53 kmh]) were relatively slower than those for other bridges (Table 1). This is ascribed to the fact that the 6th Avenue Bridge was located near curved tracks; hence, train conductors tended to reduce operating speed.

**Table 1—Summary of bridge details**

Bridge	Type	Typical cross section	Spans modeled	Materials	Speed*
Indiana Bridge	Prestressed concrete box		Five spans (628 ft [191 m])	<ul style="list-style-type: none"> <li>• Post-tensioned concrete: <math>f'_c = 5800</math> psi (40 MPa)</li> <li>• Prestressing steel: <math>f_{pu} = 270</math> ksi (1860 MPa)</li> </ul>	40.4 mph (65 km/h)
Santa Fe Bridge	Prestressed concrete box		Two spans (334 ft [102 m])	<ul style="list-style-type: none"> <li>• Post-tensioned concrete: <math>f'_c = 6000</math> psi (41 MPa)</li> <li>• Prestressing steel: <math>f_{pu} = 270</math> ksi (1860 MPa)</li> </ul>	46.0 mph (74 km/h)
County Line Bridge	Prestressed concrete girders		Four spans (580 ft [177 m])	<ul style="list-style-type: none"> <li>• All concrete: <math>f'_c = 8500</math> psi (60 MPa)</li> <li>• Prestressing steel: <math>f_{pu} = 270</math> ksi (1860 MPa)</li> </ul>	49.0 mph (78 km/h)
6th Avenue Bridge	Prestressed concrete girders		Four spans (328 ft [100 m])	<ul style="list-style-type: none"> <li>• Concrete deck: <math>f'_c = 4500</math> psi (31 MPa)</li> <li>• Post-tensioned concrete: <math>f'_c = 9000</math> psi (62 MPa)</li> <li>• Prestressing steel: <math>f_{pu} = 270</math> ksi (1860 MPa)</li> </ul>	32.9 mph (53 km/h)

\*Average train speed measured on site.

### Static model

Quadrilateral shell and three-dimensional frame elements were employed to model the bridge structures (Fig. 6(a) and (b)). Link elements were used to define connections between the components such as bridge girders and bearings. All geometric and material properties (Fig. 1 and Table 1) were nominal and nonlinearity was not taken into account. The built-in automatic meshing options generated the bridge models. When expansion joints are presented in a continuous system (that is, physical separation of the bridge girders), the portion of the continued superstructure was modeled without considering other portions. The reason is that the behavior of the modeled portion was not influenced by the other portions owing to the separation: the rail part can provide minor connectivity, whereas its effect is negligible from a structural standpoint. The condition of expansion bearings on site may have partial fixity, when loaded in longitudinal bending; however, insufficient information was available to represent this partial fixity. The models were thus developed with ideal rollers. Perfect connection between the elements was assumed, which is typical in bridge modeling and analysis, because the bridges have full composite action. Following the engineering drawings of each bridge, the translational degrees of freedom of supports at individual piers and abutments were restrained. Diaphragms were also included to prevent global torsional buckling of the girders. The dead load of each constituent element was considered by including the density of the materials: concrete (150 lb/ft<sup>3</sup> [2400 kg/m<sup>3</sup>]), ballast (120 lb/ft<sup>3</sup> [1920 kg/m<sup>3</sup>]), and rail track (200 lb/ft [3 kN/m]). According to literature,<sup>13</sup> the effects of a ballast layer were modeled with equivalent uniaxial stiffness (6854 kip/ft [100 MN/m]) and damping (5.6 kip-s/ft [82 kN-s/m]). These ballast elements were placed underneath the rails. Various load scenarios were modeled: one-track loaded, two-track loaded, and both-track loaded with two to three articulated light rail trains, as observed in the field.

### Dynamic model

Time-history analysis was performed to predict the dynamic behavior of the bridges (Fig. 6(c)) based on the average train speeds measured on site (Table 1). The mode superposition method was selected because it is less sensi-

tive to time steps (numerically stable) compared with the direct integration. As such, accurate technical results were attained with reasonable computational effort. Constant modal damping was used in accordance with AASHTO LRFD BDS: 2% for concrete bridges.<sup>14</sup> These values are also in an applicable range for rail bridges.<sup>15–17</sup> The train loading was regarded as a transient parameter. First five modes and corresponding frequencies were extracted using Eigenvector analysis. The fundamental frequency of each bridge model offered information necessary to assess user comfort criteria, to be described later. The five modes were iteratively calculated with the following convergence criterion

$$\frac{1}{2} \left( \frac{\mu_{i+1} - \mu_1}{\mu_{i+1}} \right) \leq 10^{-9} \quad (1)$$

where  $\mu$  is the eigenvalue relative to the frequency shift at the  $i$ -th iteration.

## RESPONSE MONITORING OF BRIDGES

This section expounds the results of field testing and model prediction associated with prestressed concrete light rail bridges. Train loadings and their effects on girder responses and serviceability are of interest.

### Temperature effect on train rails

As mentioned previously, strain gauges were bonded to measure the effects of temperature on the behavior of track rails while monitoring train load. The coefficient of thermal expansion (CTE) for steel (115RE) was taken as  $\alpha = 6.5 \times 10^{-6}/^{\circ}\text{F}$  ( $12 \times 10^{-6}/^{\circ}\text{C}$ ),<sup>18</sup> and a rail temperature ( $T$ ) was obtained from the relationship between thermal strain ( $\epsilon_{th}$ ) and CTE (that is,  $T = \epsilon_{th}/\alpha$ ). The temperature variation range of each bridge is summarized in Table 2: the maximum positive and negative temperatures denote relative changes in temperature against initial temperatures (for example, the lower bound for the Indiana Bridge was  $-5.1^{\circ}\text{F}$  [ $-2.8^{\circ}\text{C}$ ], which means that the maximum temperature drop was  $-5.1^{\circ}\text{F}$  [ $-2.8^{\circ}\text{C}$ ] from the initial temperature when the site work began). A net temperature variation for all bridges was in between 11.1 and 25.0°F (6.1 and 13.9°C), excluding the



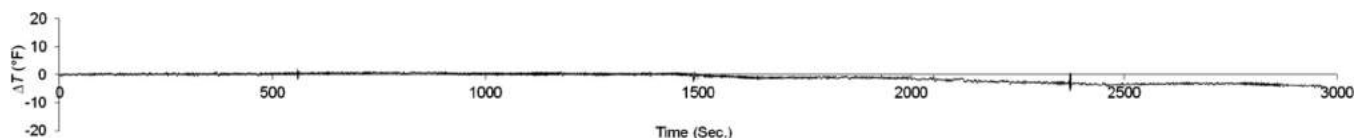


Fig. 7—Typical temperature variation of track rail measured in County Line Bridge. (Note:  $^{\circ}\text{F} = ^{\circ}\text{C}(9/5) + 32$ .)

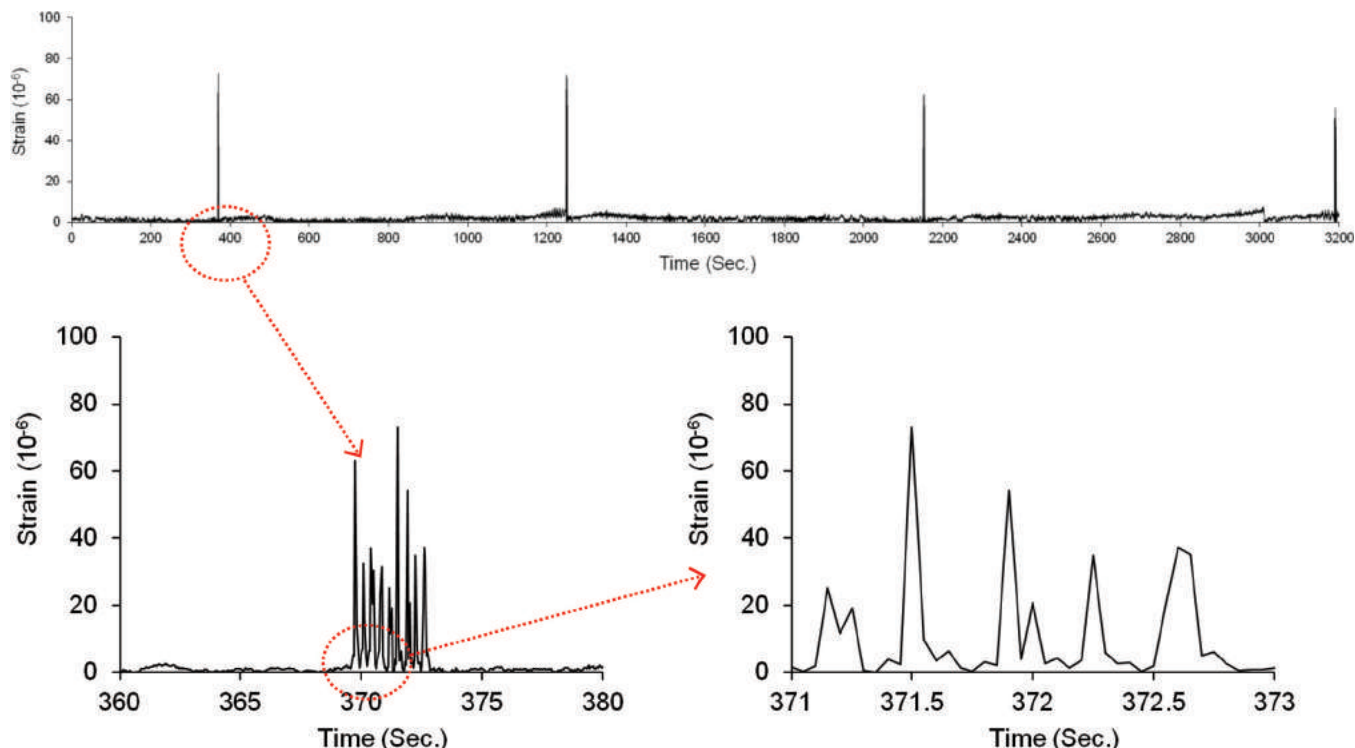


Fig. 8—Measured strains for light rail train wheel load of County Line Bridge.

**Table 2—Maximum temperature variation of monitored bridges**

Bridge	Maximum positive and negative temperatures	Net temperature variation
Indiana Bridge	−5.1°F to 19.9°F (−2.8°C to 11.1°C)	25.0°F (13.9°C)
Santa Fe Bridge	−3.5°F to 16.4°F (−2.0°C to 9.1°C)	19.9°F (11.1°C)
County Line Bridge	−8.0°F to 3.1°F (−4.4°C to 1.7°C)	11.1°F (6.1°C)
6th Avenue Bridge	−23.5°F to 9.7°F (−13.1°C to 5.4°C)*	33.2°F (18.5°C)*

\*Strong wind blew when bridge was monitored so strain reading was influenced.

temperature of the 6th Avenue Bridge, whose strain readings were influenced by strong wind blown during the 2 consecutive days when the field work was conducted (because the response of a bulb-tee superstructure was already measured in the County Line Bridge, further site monitoring for the 6th Avenue Bridge was not carried out). Train loading did not significantly affect the temperature gauge readings, because the horizontal-direction gauge was bonded at the centroid of the rail where flexural stress was none (although some minor effects were observed in the converted temperature spectra, as shown in Fig. 7).

### Wheel load of light rail trains

Figure 8 reveals typical strain responses associated with the wheel load of light rail trains running on the County Line Bridge. It is worth noting that strain reversals were corrected to exhibit consistent positive load values. The strains measured on the rail side were converted to the wheel load of the trains using the formulas developed in the laboratory test, which were also calibrated with the stationary light rail trains. When interpreting the train load, the aforementioned temperature effect was compensated. Provided that the primary interest of the present site work was in detecting maximum train loads that would control the response of the bridges (that is, the light rail train has two design loads [fully loaded) for six axles such as 24.375 and 16.25 kip [108 and 72 kN], as shown in Fig. 9(a), and corresponding wheel loads are 12.188 and 8.125 kip [54 and 36 kN]), maximum loads (or peak loads) measured during each load cycle were acquired and summarized in Fig. 9(b). It should be noted that the lower bound of the train wheel loads in Fig. 9(b) was intentionally cut to the minimum wheel load of an empty train (4.96 kip [22 kN]). The reason is that tremendous amounts of insignificant strain readings were recorded, which are considered noise rather than structural load. The number of observations (the ordinate of Fig. 9(b)) was not consistent for all bridges (Appendix B), because some bridges were used by multiple lines (there are six light rail lines in Denver); however, the

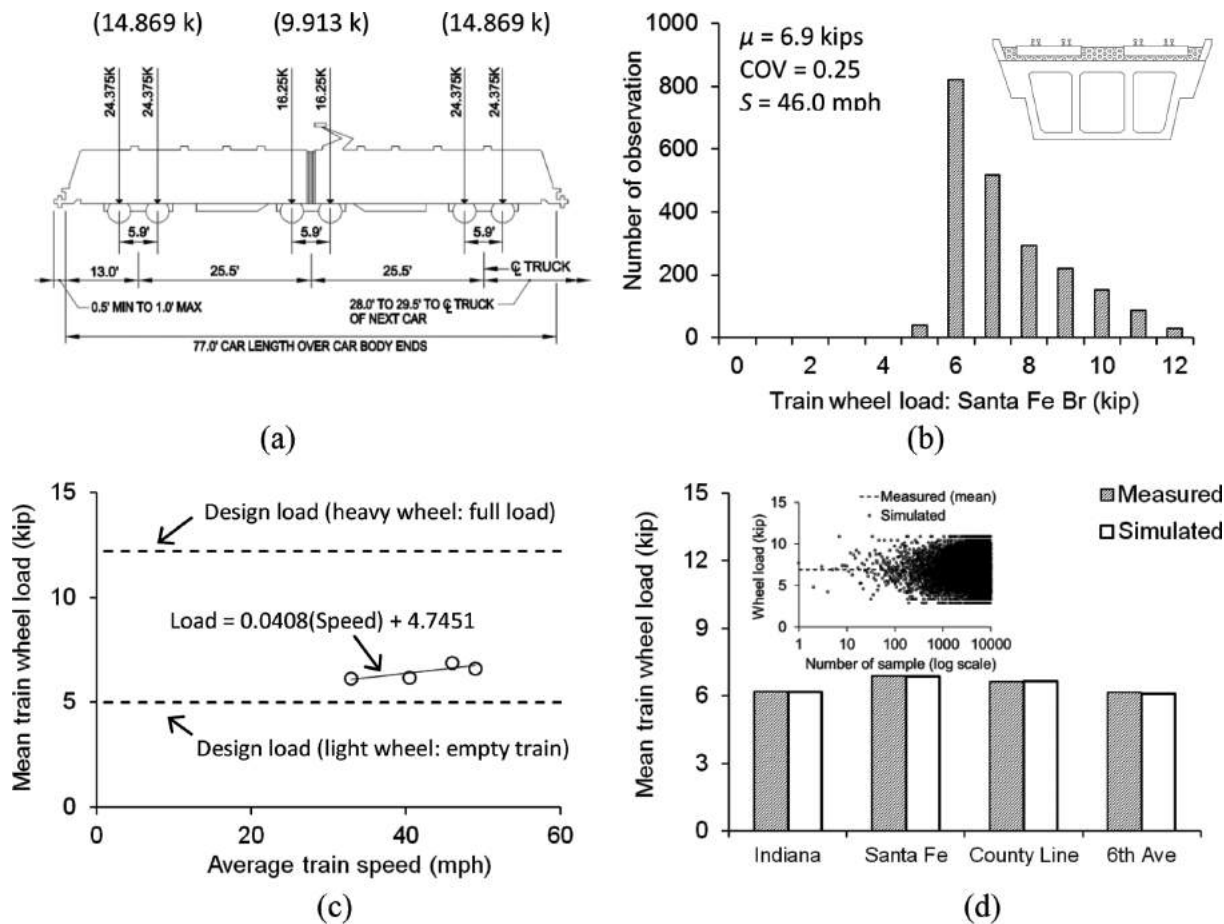


Fig. 9—Light rail train load: (a) fully loaded design axle loads (axle loads of empty train = 14.869 and 9.913 kip [66 and 44 kN]); (b) distribution of measured train wheel load ( $\mu$  = average;  $COV$  = coefficient of variation;  $S$  = average train speed); (c) mean train load measured versus average train speed; and (d) comparison between measured and predicted train wheel loads. (Note: 1 kip = 4.448 kN; 1 mph = 1.6 km/h.)

mean wheel load measured was almost consistent, irrespective of number of observations. This fact corroborates that the load data are statistically stable. The mean wheel load of the light rail trains on the monitored bridges varied from 6.2 to 6.9 kip (28 to 31 kN). The measured load range was reasonable, because the articulated light rail train had a nominal load range between 4.96 and 12.19 kip (22 and 54 kN) (empty train and fully loaded train, respectively) per train wheel (Fig. 9(a)). The passenger occupancy increased the train load, including some dynamic effects that will be examined in a subsequent section. Figure 9(c) illustrates the relationship between the average train speed measured and the mean train wheel load. In accordance with the regression line, the load has increased with train speed. Although the passenger load was not identical in the individual trains (the number of passengers is stochastic in nature), it appears to be reasonable to adopt the fitted equation because the variation range of the wheel loads was marginal (that is, 6.2 to 6.9 kip [28 to 31 kN]). The type of a probability distribution for train loading was Gaussian. A probability-based load estimate was conducted using a Monte-Carlo simulation in conjunction with the statistical properties acquired from the site (for example, coefficients of variation), as shown in Fig. 9(d). The simulated wheel loads agreed with those measured on site, including a maximum margin of 0.28%.

### Girder response

The flexural behavior of the County Line Bridge is provided in Fig. 10 (only selected cases are shown for brevity because the superstructure responses were intrinsically repeated). The measured strains at midspan of each girder showed periodic spikes when the light rail trains were passing. Some minor negative strains were detected in all cases, because the bridges were continuous and the behavior of the girders physically moved up and down depending upon the location of train load. Figure 11 compares the measured and predicted dynamic displacements at midspan of the individual bridges. For consistency, the finite element models included three cases (that is, empty and fully loaded train loads as well as typical service loading based on the empty train, plus the estimated passenger load enumerated in Table 3 with inbound train loading, which was close to the installed reflector (Fig. 5(a)). The sign convention used in Fig. 11 is as follows: positive and negative values indicate downward and upward displacements, respectively. It should be noted that the direction of train operation affected the positive and negative displacements of the monitored span in continuous bridge systems (that is, downward to upward deflections or upward to downward deflections with time in Fig. 11). The service response with average passenger loading was positioned in between the



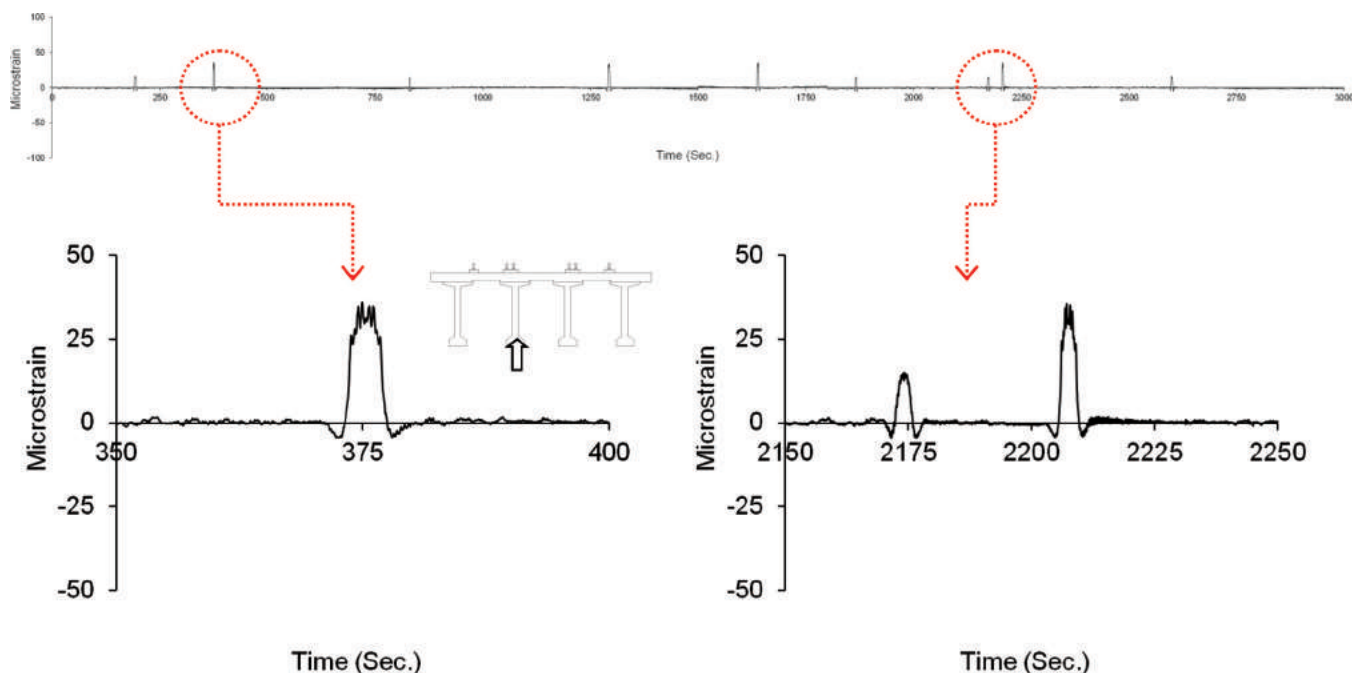


Fig. 10—Flexural response of County Line Bridge (interior girder).

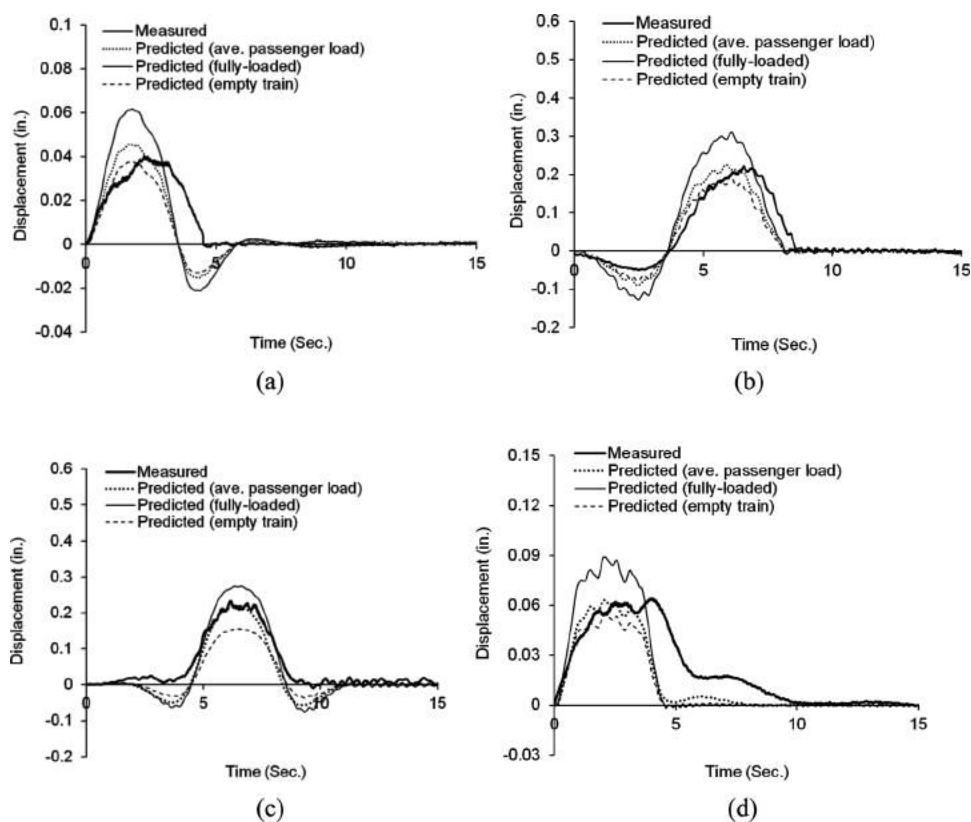


Fig. 11—Comparison between measured and predicted dynamic displacements at midspan: (a) Indiana Bridge; (b) Santa Fe Bridge; (c) County Line Bridge; and (d) 6th Avenue Bridge. (Note: 1 in. = 25.4 mm.)

fully loaded and the empty train loading cases, and the predicted service responses were in agreement with their measured counterparts.

Figures 12(a) and (b) reveal the strain response of the Indiana and the 6th Avenue Bridges (other bridge responses are available in Appendix C). The measured strain responses were generally positioned in between the fully loaded and

empty train cases of the model prediction owing to passenger loadings. It is estimated that the passenger occupancy has increased the live load of light rail trains by 23.3%, on average, leading to a dynamic train load of 97.4 kip (433 kN). The average strain readings measured on site were also compared with those predicted with typical service loadings (that is, empty train load plus the average passenger

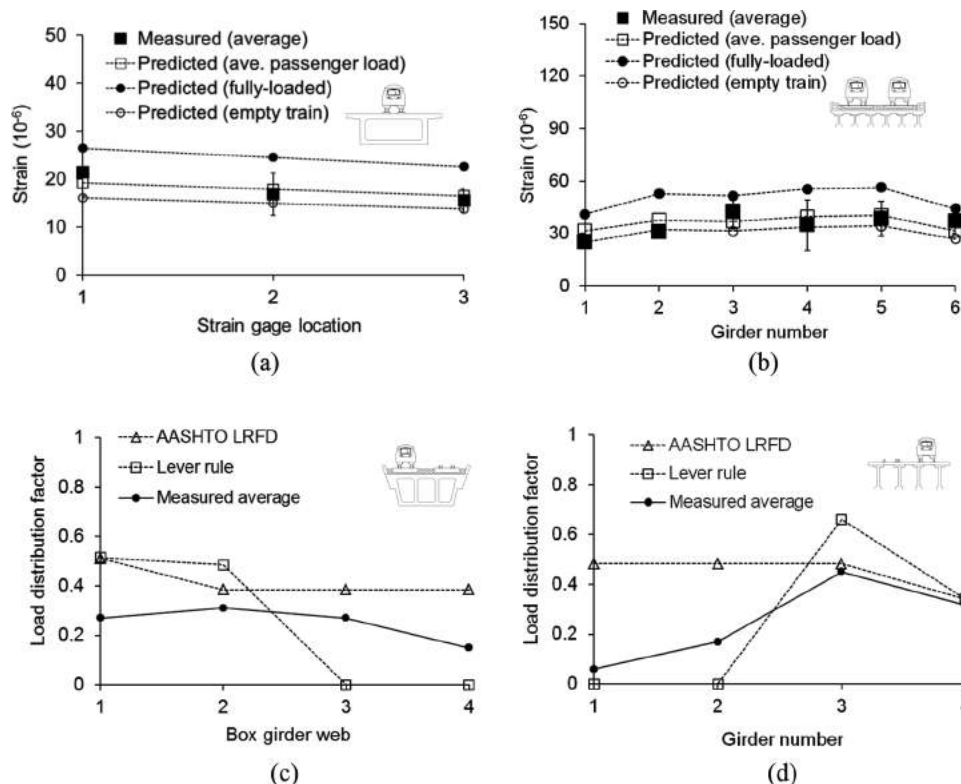


Fig. 12—Live load distribution of bridges: (a) comparison of strains in Indiana Bridge; (b) comparison of strains in 6th Avenue Bridge; (c) assessment of design approaches for Santa Fe Bridge; and (d) assessment of design approaches for County Line Bridge.

**Table 3—Average train load increase due to passenger occupancy**

Bridge	Estimated load increment due to passenger loading in service*
Indiana	Average increment: 19.5% (94.4 kip [420 kN])
Santa Fe	Average increment: 15.0% (90.9 kip [404 kN])
County Line	Average increment: 35.5% (107.0 kip [476 kN])
6th Avenue	Cannot be obtained due to strong wind

\*Increases are indicated from empty train load (79 kip [351 kN]).

load of each bridge; the passenger loading of the 6th Avenue Bridge was assumed to be the average passenger loading of the other bridges, because specific loading information was not obtained on account of the wind issue). Although some minor discrepancy was noticed, the predicted strains were within the range of the in-place strains, as shown in the vertical bars of the measured strains in Fig. 12(a) and (b). It is also important to note that passenger loading is not deterministically predictable because of its stochastic occurrence; hence, statistical properties detailed in the subsequent section will be useful to address uncertainty, when developing design recommendations.

### Live load distribution

Figures 12(c) and (d) show the load distribution factors (LDF) of selected bridges calculated by Eq. (2), depending upon the location of light rail trains

$$\text{LDF} = m \frac{I_i \varepsilon_i}{\sum_{i=1}^n I_i \varepsilon_i} \quad (2)$$

where  $m$  is the number of loaded tracks;  $I_i$  and  $\varepsilon_i$  are the moment of inertia of the cross section and the strain of the  $i$ th girder, respectively; and  $n$  is the total number of girders in the superstructure. By including the number of loaded tracks factor  $m$ , the results of beam-line analysis with a single-track-loaded case can be expanded to multiple-track-loaded cases. Live load distribution factors are controlled by the position of train wheels, rather than the gross weight of light rail trains. Table 4 lists the statistical parameters attained from the in-place tests with a focus on live load distribution (Appendix D). The averaged coefficients of variation of each bridge varied from 0.133 to 0.240, excluding the 6th Avenue Bridge that exhibited significant scatter due to the strong wind (that is, an increased level of dispersion in response). The overall average coefficient of variation for the monitored bridges was found to be 0.187.

Figures 12(c) and (d) further evaluate the application of the Lever Rule and the AASHTO LRFD BDS equations against the measured load distribution factors. These two existing approaches were by and large conservative, especially for the interior girders (Appendix E). Modified design equations for a live load distribution in light rail bridges need to be proposed to better assist practitioners. It is worth noting that the load distribution of the multiple girders, when the Lever Rule was applied to the exterior girders, was obtained from the AASHTO LRFD BDS equations and the purpose of the presentation in Fig. 12(c) and (d) was to assess the existing design approaches (governing factors are taken when a bridge is designed).

## Deflection and user comfort

The primary purpose of controlling bridge deflection is to prevent user discomfort (pedestrians and passengers) and structural deterioration induced by excessive bending. The following existing criteria for deflection control were considered:

- $L/640$  for train load (AREMA<sup>9</sup>)
- $L/800$  for vehicular load general (AASHTO LRFD BDS<sup>14</sup>)
- $L/1000$  for girders (local light rail transit agencies such as RTD<sup>12</sup>)

where  $L$  is the span-length of the bridge. The maximum average deflection of each bridge is provided in Table 5 along with the  $L/m$  criterion, where  $m$  is a constant. The  $L/m$  values of all bridges were significantly less than those mentioned earlier. This implies that the existing deflection control criteria are not sufficient to address serviceability concerns. Another criterion should, therefore, be taken into consideration—namely, the comfort of users such as pedestrians and passengers (further discussions are available in the following).

The fundamental frequencies measured and predicted are compared in Table 6. Although reasonable agreement was observed in all cases, minor discrepancy was noticed possibly because of the noise detected by the sensitive data acquisition. According to a sensitivity study using the finite element models, the effect of miscellaneous members (for example, concrete plinths and sidewalks) was negligible on the variation of fundamental frequency. Figure 13 evaluates user comfort (pedestrian) based on the deflection and fundamental frequency of the in-place bridges. The comfort criteria of the Canadian Highway Bridge Design Code (CHBDC) were adopted<sup>19</sup>: 1) frequent pedestrian use; 2) occasional pedestrian use; and 3) without pedestrians. These criteria were developed based on bridge acceleration limits, which were converted to equivalent static deflections for design purposes. The applicability of the CHBDC criteria was previously assessed in Roeder et al.<sup>20</sup> using 12 bridges designed per the AASHTO Specifications. Given that the monitored bridges have right-of-way and do not allow pedestrians for safety reasons, the third criterion was

exploited in Fig. 13. The predicted fundamental frequency and corresponding maximum deflection of the individual bridges generated specific responses, all of which were within the acceptable zone of user comfort. These observations support the fact that the serviceability of the in-place light rail bridges was satisfactory in terms of deflection (Table 5) and user comfort (Fig. 13).

The International Union of Railways (UIC Code 776-2<sup>21</sup>) employs bridge deflection as a measure of passenger comfort, and provides three comfort levels based on the vertical acceleration of railway bridges (1.0, 1.3, and 2.0 m/s<sup>2</sup> [39, 51, and 79 in./s<sup>2</sup>] for the Very good, Good, and Acceptable levels, respectively). The deflection limit equivalent to the Very good category is  $L/600$ <sup>21</sup> for bridges carrying trains operating at 60 mph (96 kmh). As examined in Table 5, the bridge deflections were within the  $L/600$  limit and, thus, passenger comfort does not seem to be a concern for light rail bridges. Design recommendations can be made in such a way that user comfort (pedestrians and passengers) may not be critical for light rail bridges when primarily subjected to train loading, whereas care should be exercised to check the pedestrian comfort requirements if a light rail bridge is intended for frequent pedestrian use as part of serviceability limit states.

## SUMMARY AND CONCLUSIONS

This paper has evaluated prestressed concrete bridges subjected to light rail transit. Four bridges in Denver, CO, were tested to examine static and dynamic responses when loaded, in conjunction with three-dimensional finite element analysis. A laboratory experiment established the relationship between rail strains and train loadings for weigh-in-motion, confirmed by additional field testing. The superstructure responses of the light rail bridges were quantified by strain gauges and non-contact interferometric radar with an emphasis on flexural behavior, passenger occupancy, statistical properties, live load distributions, natural frequencies, and user comfort. The design provisions of existing specifications were assessed. The following conclusions are drawn:

- The measured train loadings were statistically stable and varied from 6.2 to 6.9 kip (28 to 31 kN), and their probability distribution was Gaussian. With an increase in train speed ranging between 32.9 and 49.0 mph (53 and 78 kmh), the train load rose by 10.8%. The stochastic passenger loading in light rail trains also increased the live load by 23.3%, on average.
- Live load distributions estimated by the Lever Rule and the equations specified in AASHTO LRFD BDS were conservative (overly conservative for interior girders) when compared with site-based distributions. To facili-

**Table 4—Average coefficient of variation (COV) for live load distribution**

Bridge	Type	COV	Average
Indiana	Prestressed concrete box (single cell)	0.133	0.187*
Santa Fe	Prestressed concrete box (multiple cell)	0.240	
County Line	Prestressed concrete girder	0.190	
6th Avenue	Prestressed concrete girder	0.351	

\*COV of 6th Avenue Bridge was not included due to heavy wind issue.

**Table 5—Assessment of deflection control**

Bridge	Type	Monitored span	Test		Model			
			Service load		Empty train		Fully-loaded train	
			$\delta_{max-average}$	$\delta_{control}$	$\delta_{max}$	$\delta_{control}$	$\delta_{max}$	$\delta_{control}$
Indiana	PC box girder	95 ft (29 m)	0.040 in. (1.0 mm)	$L/28,500$	0.038 in. (0.9 mm)	$L/30,000$	0.062 in. (1.6 mm)	$L/18,390$
Santa Fe	PC box girder	155 ft (47 m)	0.224 in. (5.7 mm)	$L/8300$	0.194 in. (4.9 mm)	$L/9590$	0.311 in. (7.9 mm)	$L/5980$
County Line	PC I girder	160 ft (49 m)	0.250 in. (6.4 mm)	$L/7680$	0.156 in. (3.9 mm)	$L/12,310$	0.274 in. (6.9 mm)	$L/7010$
6th Avenue	PC I girder	80 ft (24 m)	0.066 in. (1.7 mm)	$L/14,550$	0.054 in. (1.4 mm)	$L/17,780$	0.089 in. (2.3 mm)	$L/10,790$



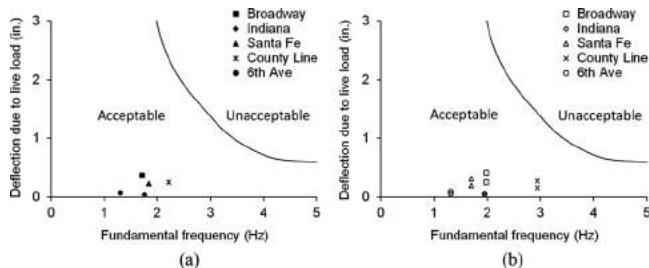


Fig. 13—Evaluation of user comfort (pedestrian): (a) average test data with service train load; and (b) model prediction with empty and fully loaded light rail trains loads. (Note: 1 in. = 25.4 mm.)

**Table 6—Comparison between measured and predicted fundamental frequencies**

Bridge	Fundamental frequency	
	Measured	Predicted
Indiana	1.76 ± 0.50 Hz	1.95 Hz
Santa Fe	1.84 ± 0.13 Hz	1.70 Hz
County Line	2.22 ± 0.85 Hz	2.95 Hz
6th Avenue	1.31 ± 0.11 Hz	1.32 Hz

tate bridge design, live load distribution factors for light rail trains should be developed or the AASHTO equations may be recalibrated to meet their loading characteristics. The average coefficient of variation of the in-place live load distribution was 0.187. Existing criteria for deflection control were not usable for light rail bridges.

- An assessment on the serviceability of the bridges clarified that user comfort (pedestrians and passengers) was not a concern for light rail transit systems. Nonetheless, if a light rail bridge accommodates frequent pedestrians, a refined analysis appears to be necessary to avoid serviceability problems.

## AUTHOR BIOS

**Yail J. Kim, FACI**, is President of the Bridge Engineering Institute, An International Technical Society, and a Professor in the Department of Civil Engineering at the University of Colorado Denver, Denver, CO. He is Chair of ACI Subcommittee 440I, FRP-Prestressed Concrete, and past Chair of ACI Committee 345, Concrete Bridge Construction and Preservation. He is a member of ACI Committees 342, Evaluation of Concrete Bridges and Bridge Elements; 440, Fiber-Reinforced Polymer Reinforcement; and Joint ACI-ASCE Committee 343, Concrete Bridge Design. He is the recipient of the Chester Paul Siess Award for Excellence in Structural Research in 2019. His research interests include advanced composite materials for rehabilitation, structural informatics, complex systems, and science-based structural engineering, including statistical, interfacial, and quantum physics.

ACI member **Yongcheng Ji** is a PhD Candidate in the Department of Civil Engineering at the University of Colorado Denver, Denver, CO. He received BS and MS from Heilongjiang University and Northeast Forestry University, Harbin, China, in 2009 and 2012, respectively. He is a member of ACI Committee 345, Concrete Bridge Construction and Preservation. His research interests include material characterization, rail structures, and bridge engineering.

## ACKNOWLEDGMENTS

The authors gratefully acknowledge financial support from the National Academy of Sciences through the National Cooperative Highway Research Program. The Regional Transportation District (RTD) and Olson Engineering in Denver, CO, provided technical assistance for this research project. It is noted that the contents of this manuscript have been excerpted

from a technical report submitted to the National Academy of Sciences under the approval of the program manager for technology transfer.

## REFERENCES

1. TRB, *Track Design Handbook for Light Rail Transit*, second edition, Transportation Research Board, Washington, DC, 2012.
2. Black, A., "The Recent Popularity of Light Rail Transit in North America," *Journal of Planning Education and Research*, V. 12, No. 2, 1993, pp. 150-159. doi: 10.1177/0739456X9301200210
3. Liu, K.; Reynders, E.; De Roeck, G.; and Lombaert, G., "Experimental and Numerical Analysis of a Composite Bridge for High-Speed Trains," *Journal of Sound and Vibration*, V. 320, No. 1-2, 2009, pp. 201-220. doi: 10.1016/j.jsv.2008.07.010
4. Lu, Y.; Mao, L.; and Woodward, P., "Frequency Characteristics of Railway Bridge Response to Moving Trains with Consideration of Train Mass," *Engineering Structures*, V. 42, 2012, pp. 9-22. doi: 10.1016/j.engstruct.2012.04.007
5. Moreu, F.; Jo, H.; Li, J.; Kim, R. E.; Kimmle, A.; Scola, S.; Le, H.; Spencer, B. F.; and LaFave, J. M., "Dynamic Assessment of Timber Railroad Bridges Using Displacements," *Journal of Bridge Engineering*, ASCE, V. 20, No. 10, 2015, p. 04014114 doi: 10.1061/(ASCE)BE.1943-5592.0000726
6. Yuan, R. L.; Bourland, M.; and Ugarte, E., "Health Monitoring of Light-Rail Aerial-Structural System," Proceedings of SPIE 4702, Smart Nondestructive Evaluation for Health Monitoring of Structural and Biological Systems, San Diego, CA, 2002, pp. 262-271.
7. Khan, E.; Linzell, D. G.; Frankl, B. A.; Lobo, J. A.; and Lozano, S., "Field Measured Dynamic Effects and Load Distribution in a Prestressed Concrete Light Rail Bridge," *Proceedings of the 2016 Joint Rail Conference (JRC 2016)*, American Society of Mechanical Engineers, Article No. JRC2016-5765, 2016.
8. AASHTO, *AASHTO LRFD Bridge Design Specification*, sixth edition, American Association of State Highway and Transportation Officials, Washington, DC, 2012.
9. AREMA, *Manual for Railway Engineering: Vol. 1-4*, American Railway Engineering and Maintenance-of-Way Association, Lanham, MD, 2015.
10. Bayoğlu Flener, E., and Karoumi, R., "Dynamic Testing of a Soil-Steel Composite Railway Bridge," *Engineering Structures*, V. 31, No. 12, 2009, pp. 2803-2811. doi: 10.1016/j.engstruct.2009.07.028
11. Remennikov, A. M., and Kaewunruen, S., "A Review of Loading Conditions for Railway Track Structures due to Train and Track Vertical Interaction," *Structural Control and Health Monitoring*, V. 15, No. 2, 2008, pp. 207-234. doi: 10.1002/stc.227
12. RTD, "Light Rail Design Criteria," Regional Transit District, Denver, CO, 2013.
13. Nielsen, J. C. O., "High-Frequency Vertical Wheel-Rail Contact Forces—Validation of a Prediction Model by Field Testing," *Wear*, V. 265, No. 9-10, 2008, pp. 1465-1471. doi: 10.1016/j.wear.2008.02.038
14. AASHTO, *AASHTO LRFD Bridge Design Specification (7th edition with 2016 interim revisions)*, American Association of State Highway and Transportation Officials, Washington, DC, 2016.
15. Ju, S. H., "Finite Element Analysis of Structure Borne Vibration from High-Speed Train," *Soil Dynamics and Earthquake Engineering*, V. 27, No. 3, 2007, pp. 259-273. doi: 10.1016/j.soildyn.2006.06.006
16. Kim, S.-I., "Experimental Evaluations of Track Structure Effects on Dynamic Properties of Railway Bridges," *Journal of Vibration and Control*, V. 17, No. 12, 2011, pp. 1817-1826. doi: 10.1177/1077546310385264
17. Martínez-Rodrigo, M. D.; Lavado, J.; and Museros, P., "Dynamic Performance of Existing High-Speed Railway Bridges under Resonant Conditions Retrofitted with Fluid Viscous Dampers," *Engineering Structures*, V. 32, No. 3, 2010, pp. 808-828. doi: 10.1016/j.engstruct.2009.12.008
18. Okelo, R., and Olabimtan, A., "Nonlinear Rail-Structure Interaction Analysis of an Elevated Skewed Steel Guideway," *Journal of Bridge Engineering*, ASCE, V. 16, No. 3, 2011, pp. 392-399. doi: 10.1061/(ASCE)BE.1943-5592.0000163
19. CAN/CSA-S6-06, "Canadian Highway Bridge Design Code," CSA International, Toronto, ON, Canada, 2006.
20. Roeder, C. W.; Barth, K.; and Bergman, A., "Improved Live Load Deflection Criteria for Steel Bridges (NCHRP 20-7)," Transportation Research Board, Washington, DC, 2002.
21. UIC, "Design Requirements for Rail-Bridges Based on Interaction Phenomena between Train, Track and Bridge (UIC Code 776-2)," International Union of Railways, Paris, France, 2009.